Journal of Manufacturing Processes 33 (2018) 43–53

Contents lists available at ScienceDirect

Journal of Manufacturing Processes

journal homepage: www.elsevier.com/locate/manpro

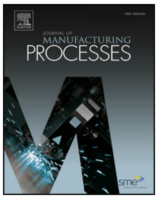

Effect of magnesium content on keyhole-induced porosity formation and distribution in aluminum alloys laser welding

Lijin Huang[a,b], Xueming Hua[a,b,*], Dongsheng Wu[a,b,*], Li Fang[a,b], Yan Cai[a,b], Youxiong Ye[c]

[a] *Shanghai Key Laboratory of Material Laser Processing and Modification (Shanghai Jiao Tong University), Shanghai 200240, PR China*
[b] *Collaborative Innovation Center for Advanced Ship and Deep-Sea Exploration, Shanghai, 200240, PR China*
[c] *Department of Materials Science and Engineering, University of Tennessee, Knoxville, TN, 37996, USA*

ARTICLE INFO

Keywords:
Laser welding
Aluminum alloy
Keyhole-induced porosity

ABSTRACT

With the aid of transparent glass, the keyhole behavior and porosity formation are directly observed in laser welding of different aluminum alloys. A three-dimensional model is developed to investigate the recoil pressure change. The influences of Mg element on porosity formation and distribution are discussed based on both numerical and experimental results. During laser welding of aluminum alloys, the molten metal in the front keyhole wall is thick. However, with the increasing Mg content, the weld depth increases in the welding direction, and longer time is required to reach the quasi-steady state; besides, the keyhole is more stable, and less keyhole-induced porosity is formed. Based on pressure balance acting on the keyhole wall, the high recoil pressure contributes to the stability of the keyhole, resulting in the suppression of porosity. Higher density of porosity is formed at the middle and bottom of the weld due to the easier collapse of keyhole in the respective regions in laser welding of aluminum alloys with higher Mg content.

1. Introduction

Aluminum alloys have been widely applied in aerospace, automobile, pressure vessel, and shipbuilding industry due to their low specific weight, good weldability and excellent corrosion resistance [1]. Compared to traditional welding methods, laser welding has advantages of high efficiency, low heat input, and high welding quality, which has attracted substantial research attention [2–4]. However, porosity is one of the main issues in laser welding of aluminum alloy, which would deteriorate the mechanical properties of welded joints, especially the tensile strength [5,6]. Therefore, it is essential to understand the porosity formation mechanism and its remission procedures during laser welding.

There are two different types of porosity in laser welding, called hydrogen-induced and keyhole-induced porosity. The formation of hydrogen-induced porosity stems from largely different hydrogen solubilities in liquid and solid metals [7]. Pastor et al. [8] joined thin plates of 5754 and 5182 aluminum alloys, and concluded that hydrogen-induced porosity was not an important issue. The keyhole-induced porosity formation in laser welding is quite different from hydrogen-induced porosity. Sun and Meng [9,10] pointed out that the formation of keyhole-induced porosity is in connection with an unstable keyhole.

It is difficult to directly observe the weld pool and keyhole in laser welding using the optical microscope. At present, the dynamic behaviors of keyhole and weld pool have been performed by means of high-speed CCD filming and spectrometer. Aalderink et al. [11] developed a camera-based in situ monitoring system to study the influence of welding modes on porosity formation during laser welding of AA5182 alloy sheets, and found that the shape of the elliptical keyhole was more susceptible to porosity. Sun et al. [12] used a high-speed video camera to observe the laser keyhole and liquid melt pool in 10 kW laser welding of 304 stainless steel, and found that there was no plume when the keyhole was closed, which could reveal the periodic closures of the keyhole. However, some useful details are not observable with the conventional methods, such as the fluctuation of keyhole, size and shape of the weld pool, and the frequency of keyhole collapse. A welding experiment [13] conducted using transparent glasses with low cost, high speed and resolution provided a better understanding of the porosity formation of aluminum alloy laser welding. However, laser welding experiments with transparent glasses were rarely carried out to observe the keyhole behaviors in fiber laser welding of aluminum alloys.

Researches about the keyhole-induced porosity were mainly focused on the effect of various parameters in the same material, such as Xu's work on welding speed and laser power [14], and Seto's work on

---

[*] Corresponding author at: Shanghai Key Laboratory of Material Laser Processing and Modification (Shanghai Jiao Tong University), Shanghai 200240, PR China.
E-mail address: xmhua@sjtu.edu.cn (X. Hua).

https://doi.org/10.1016/j.jmapro.2018.04.023
Received 28 January 2018; Received in revised form 18 April 2018; Accepted 29 April 2018

shielding gas [15]. Lin et al. [16] developed a three-dimensional model using the multi-reflection and Fresnel absorption of laser beam in the keyhole to investigate keyhole dynamics and melt flow in AA5182 aluminum alloy laser welding with a thickness of 2 mm, and proposed that the laser inclination angle could suppress the porosity formation by preventing the keyhole collapse. Li et al. [17] optimized welding parameters to eliminate the porosity in laser welding of A356 aluminum alloy. Masanori et al. [18] suggested that a stable keyhole with a porosity rate of 6% could be obtained, attributed to the slight heat input variation caused by the fan usage in laser welding of pure Al. However, owing to the different magnesium (Mg) element contents in different aluminum alloys, keyhole-induced porosity formation and distribution are different in aluminum alloys laser welding. The vaporization of volatile alloying elements such as Mg is an important issue during laser welding process [19]. Haboudou et al. [20] joined AA5083 and A356 aluminum alloy of 4 mm in thickness via laser welding, and found that much more porosity was generated in AA5083 aluminum alloy. The boiling point of Mg (1360 K) is larger than the melting point of Al (933 K) but much lower than the boiling point of Al (2723 K), so more Mg element is evaporated and escapes from the weld pool in aluminum alloy laser welding. However, the effect of Mg content on keyhole behavior and keyhole-induced porosity formation has not yet been well addressed, and few researches were focused on the keyhole-induced porosity distribution in various aluminum alloys laser welding.

In this study, laser welding experiments of 1050, 6061, 2A12, 5754, 5083 and 5A06 aluminum alloys with transparent glasses were performed to directly observe the shape of weld pool and the fluctuation of keyhole by a high-speed video camera. A three-dimensional model is developed to investigate the recoil pressure change. Based on experimental investigation and numerical study, the relationship between the Mg content in the weld and the keyhole-induced porosity formation mechanism is revealed in detail, and the quantity and distribution tendency of keyhole-induced porosity formation are also analyzed in laser welding of various aluminum alloys.

2. Experimental procedure

The experimental set-up is shown in Fig. 1. The experiments are carried out by a fiber laser system with the wavelength of 1.070 ± 0.010 mm, the rayleigh length of 10.328 mm, and the beam parameter product of 12.5 mm mrad (IPG YLS-10000; focus radius: 0.36 mm; maximum output power: 10 kW). The base material used in this study are 1050, 6061, 2A12, 5754, 5083 and 5A06 plates in the dimension of 100(L) × 30(W) × 10 mm(H), and heat resistant quartz glass in the dimension of 100(L) × 10(W) × 10 mm(H). The chemical compositions of the base metal and glass are given in Table 1, and the thermo-physical material properties of aluminum alloys are summarized in Table 2.

Table 1
Chemical composition of aluminum alloys and glass (wt.%).

Materials	Elements,wt.%							
	SiO_2	Fe	Si	Mn	Mg	Ti	Zn	Al
1050	–	0.4	0.25	0.05	0.05	0.03	0.05	Bal.
6061	–	0.7	0.4–0.8	0.15	0.8–1.2	0.15	0.25	Bal.
2A12	–	0.5	0.5	0.3–0.9	1.2–1.8	0.15	0.3	Bal.
5754	–	0.4	0.4	0.5	2.6–3.6	0.15	0.2	Bal.
5083	–	0.4	0.4	0.4–1.0	4.0–4.9	0.25	0.25	Bal.
5A06	–	0.4	0.4	0.5–0.8	5.8–6.8	0.02–0.1	0.2	Bal.
Glass	99.97–99.99	–	–	–	–	–	–	–

Table 2
Thermo-physical material properties of aluminum alloys.

Materials	Density, $\mathrm{Kg\,m^{-3}}$	Thermal conductivity, $\mathrm{W\,m^{-1}\,k^{-1}}$	Melting temperature, K
1050	2.70	231	933
6061	2.72	180	924
2A12	2.75	193	904
5754	2.68	134	887
5083	2.66	90	847
5A06	2.68	117	843

Prior to welding experiments, all specimens are carefully brushed by stainless steel brush, and cleaned by acetone to wipe off the oxidation film. The welding is performed under a laser power of 6 kW with a defocused distance of 0 mm in a speed of 2 m/min. Pure argon gas is used as shielding gas with a flow rate of 20 L/min, and an 8 mm diameter shielding gas nozzle at an inclination of 45° is used to protect the weld.

A high speed CCD (Photron VEO 710S) together with a band pass filter with a transmission band of 640 nm is placed at different positions to detect the keyhole and weld pool behaviors. The computer and high-speed video camera must be associated with the same sub-network to communicate with one another, and this process is carried out with a laser-assisted light (Cavilux Smart) to illuminate the weld to obtain clear images. Images are recorded at a speed of 5000 frames/s.

After welding, the porosity in the weld is examined using X-ray radiography. The metallurgical samples of weld transverse and

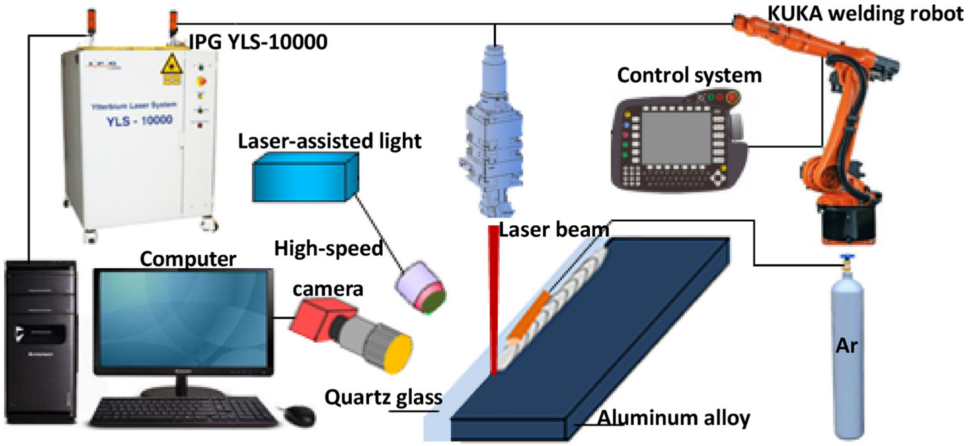

Fig. 1. Diagram of the experimental platform.